Results in Chemistry 7 (2024) 101519

Contents lists available at ScienceDirect

Results in Chemistry

journal homepage: www.sciencedirect.com/journal/results-in-chemistry

Supported silver nanoparticles over Metronidazole modified-single walled carbon nanotubes for overcoming anti-microbial properties, anti-cancer effect, and apoptosis induction on human gastric cancer cell line

Shirin Mahmoudi [a], Maryam Otadi [a,*], Malak Hekmati [b,**], Majid Monajjemi [a], Azadeh Sadat Shekarabi [a]

[a] Department of Chemical Engineering, Central Tehran Branch, Islamic Azad University, Tehran, Iran
[b] Department of Organic Chemistry, Faculty of Pharmaceutical Chemistry, Tehran Medical Sciences, Islamic Azad University, Tehran, Iran

ARTICLE INFO

Keywords:
Carbon Nanotubes
Silver Nanoparticle
Antibacterial
Anticancer
Metronidazole

ABSTRACT

One of the most important goals of current research in the medical field is to identify treatments for antimicrobial resistance (AMR) and cancer. The latest developments in nanotechnology have provided opportunities to develop novel nanomaterials that can overcome the limitations of current treatments. In this regard, carbon nanotubes (CNTs) are considered potential nano-tools with attractive implications. The analysis of MTZ/SWCNT/AgNPs in this study was done using different techniques, including SEM, TEM, FTIR, XRD, and EDX. Antibacterial activity was assessed for MTN/SWCNT/AgNPs against *Escherichia coli*, *Pseudomonas aeruginosa*, *Enterococcus faecalis*, and *Staphylococcus aureus*. The effects of MTZ/SWCNTs/AgNPs on mitochondrial and apoptotic activities in human gastric cancer (AGS) were evaluated. Overall, new CNTs were produced efficiently. MTZ/SWCNTs/AgNPs are considered efficient antibacterial and anticancer agents for biological applications.

1. Introduction

Microorganisms [1] and cancer [2] have been a major challenge for the global healthcare system over the last several decades. Antimicrobial resistance (AMR) instances are rising owing to the overuse and abuse of antibiotics, which have rendered them ineffective [3–5]. Current cancer therapies, such as surgery, radiation, chemotherapy, or a combination of the three, are associated with many side effects that significantly influence the patient's quality of life [6,7]. Recent research indicates that like bacteria, tumors can develop drug resistance, resulting in a novel form of chemotherapy-resistant cancer cells [8,9]. Therefore, cancer and AMR require an instant answer that departs significantly from our overgrown reliance on present and antiquated standard therapies.

Researchers are interested in new compounds with antibacterial and anticancer characteristics including metallic nanoparticles (MNPs). MNPs, especially silver nanoparticles (AgNPs), with useful functions have attracted interest in biomedical applications [10,11]. Based on thorough antimicrobial investigations, these NPs have been utilized in wound healing ointments [12], bandage cloths [13], dental work [14], and food packaging [15]. Recent studies have focused on the biological uses of AgNPs, including drug delivery systems and cancer treatment [16,17]. Composite nanomaterials are in high demand because they increase their biological activity and satisfy certain parameters. In this regard, carbon nanotubes (CNTs) can offer the optimal substrate for hosting and/or conjugating bioactive compounds with MNPs [18].

CNTs are formed by sp2-hybrid carbon atoms that are organized into a hexagonal mesh measuring nanometers [19]. Due to their high specific surface area, thermal conductivity, mechanical stability, and rich surface potential, biomedical applications have focused on these materials [20–22]. Regarding this, functionalized CNTs deliver chemotherapeutic agents, genes, and proteins [23,24]. In one type of classification, carbon nanotubes can be classified into two categories: SWCNT and MWCNT. Single-walled carbon nanotubes consist of a single layer of graphene, which is in the shape of a tube, and MWCNTs consist of several cylindrical graphene layers coaxially with each other [25]. Until now, numerous studies have used SWCNTs and MWCNTs for targeted delivery of antibacterial [26,27] and anticancer agents [28–31]. Ahmad et al. demonstrated that SWNTs/TiO2/Ag and MWNTs/TiO2/Ag could

* Corresponding author.
** Corresponding author.
E-mail addresses: m-otadi@iauctb.ac.ir (M. Otadi), mhekmatik@yahoo.com (M. Hekmati).

https://doi.org/10.1016/j.rechem.2024.101519
Received 18 March 2024; Accepted 24 April 2024
Available online 6 May 2024

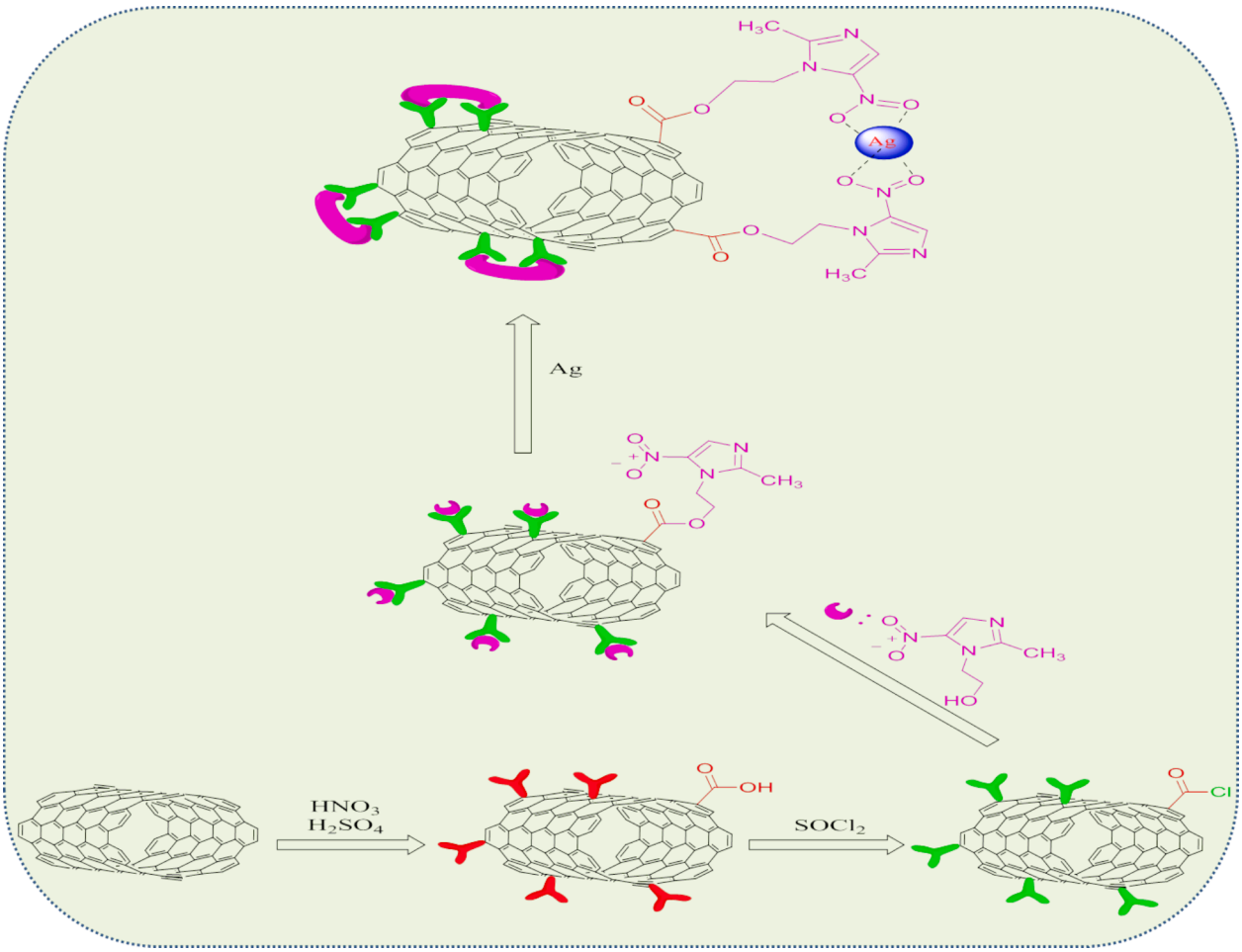

Scheme 1. The schematic preparation procedure of MTZ/SWCNTs/AgNPs.

specifically target uterine cancer (SiHa) cells while impacting normal (WRL68) cells much less [32]. In a mouse model of hepatic cancer, it was shown that MWCNTs conjugated with 10-hydroxy camptothecin (MWCNTs/HCPT) had a more potent anticancer effect than the therapeutic version of HCPT [33]. Dinh et al. evaluated the antibacterial activities of MWCNTs, AgNPs, and MWCNTs/Ag samples towards Staphylococcus aureus and *Escherichia coli*. This indicated that MWCNTs/Ag possessed higher antibacterial activity than MWCNTs [26]. On the other hand, CNTs have low solubility, aggregation, and cytotoxicity, which limits their applicability. Surface modification is essential for improving the solubility, biocompatibility, penetration, and cytotoxicity of biological systems [34].

New synthesis methods for silver nanoparticles are important due to their ability to be used as powerful antibacterial agents, specifically against Bacillus subtilis, Escherichia coli, Staphylococcus aureus, Pseudomonas aeruginosa, In addition to Micrococcus flavus, Klebsiella and pneumoniae, Bacillus pumilus is also an effective factor against human cancer cells like A549 lung cancer [35], PC-3 prostate cancer [36], A431 skin cancer [37], HeLa cervical cancer [38], colon cancer cells [39], and Hep-G2 liver cancer cells[40].

Majid et al showed that being exposed to SWCNTs and SWCNTs@Ag–TiO_2 substance adjusts the ROS indicating nerve tract in Hep-G2 human liver cancer cell line, leading to the inductance of apoptosis and autophagy. Their findings resulted in producing more powerful drugs to treat human liver cancer [41]. Rahimi et al synthesized Ag-ZnO nanoparticles using the sol–gel method in another study. The photocatalytic and antibacterial activity of Ag-ZnO nanoparticles, which were synthesized, was evaluated against opportunistic skin pathogens. Besides, ex vivo studies were conducted to investigate the anticancer features of Ag-ZnO nanoparticles against UVB-induced human keratinocytes. The produced Nanoparticles showed a considerable photocatalytic activity towards Ponceau, with a maximum degradation of 89 %. Furthermore, Ag-ZnO nanoparticles were found to be exhibiting good bactericidal activity towards opportunistic skin pathogens. Ag-ZnO nanoparticles exhibit strong photocatalytic, antibacterial, and anticancer activity, resulting in apoptosis and the death of UVB-evoked cancer cells [42]. Pratiosa et al studied how HSA interacts with AgNPs coated with quercetin to reverse multidrug resistance (MDR). Reversing MDR in cancer treatment can be beneficial, and this type of nanoparticles may be capable of acting as an antibacterial as well as an anticancer agent at the same time [43].

The preparation of MWCNT-Ag nanocomposite membrane coated with polyphenylsulfone as nano absorbent and effective antimicrobial agents has been reported by Shukla et al. The findings showed that adding MWCNT-Ag substantially increased the efficiency of selective removal of heavy metal ions by this nano absorbent. In addition, the antibacterial capability of nanocompos te was examined against Escherichia coli and Staphylo had *a significant role of Ag-MWCNT in ameliorating the antibacterial properties of the s*ynthetic nanocomposite [44]. Huang et al. demonstrated that synthesis of carbon nanotube/polyamide nanofibers doped with Ag nanoparticles (Ag@CNT/PA). Their results showed that silver nanoparticles are homogeneously dispersed on the surface of nanofibers. In addition, the thermic conduction ability of Ag@CNT/PA nanocomposite is significantly improved in comparison with polyamide nanofibers. In addition, Ag@CNT/PA nanocomposite has shown excellent antibacterial activity against gram-

positive and negative bacteria. Therefore, synthetic nanofibers can be used as new antibacterial materials [45]. In another research study, the antibacterial properties of SWCNT nanocomposite functionalized with Ag and TiO2 nanoparticles have been evaluated against Staphylococcus aureus and Escherichia coli. The results have shown that the synthetic nanocomposite has strong antibacterial activity against both bacteria. Phyllo coccus has shown less sensitivity to this nanocomposite compared to Escherichia coli [46].

Metronidazole (MTZ) is a multifunctional candidate for the modification of SWCNT/AgNPs [47]. Growing evidence indicates that MTZ has anticancer capabilities in addition to its antibacterial action [48,49]. This study intended to develop MTZ-modified SWCNTs loaded with AgNPs (Scheme 1). To the best of our understanding, relatively few investigations have been conducted on the antibacterial and anticancer effects of biohybrid materials. Various physical–chemical properties of MTZ/SWCNTs/AgNPs nanocomposite were characterized using different methods including FT-IR, FE-SEM, TEM, XRD, and EDX. In addition to possessing antibacterial properties, these synthesized biohybrid materials exhibit anticancer effectiveness against human gastric adenocarcinoma (AGS).

2. Substances and approaches

2.1. Substances

All the materials used were supplied by valid and well-known chemical companies such as Merck and Sigma-Aldrich and were utilized with no refinement. Pristine SWCNTs were purchased from Petrol Chemical Co. (Tehran, Iran). Merck and Sigma-Aldrich provided the research with all required materials, including deionized (DI) water, silver nitrate (AgNO3), hydrochloric acid (HCl), dimethyl formamide (DMF), sulfuric acid (H_2SO_4), THF, $SOCl_2$, and $NaBH_4$.

2.2. Characterization of MTZ/SWCNTs/AgNPs

A Perkin Elmer 65 spectrometer was employed to document FTIR spectra in the 400 to 4000 cm-1 range using pressed KBr disks. CuK was used in a Bruker D8 Advance diffractometer to carry out XRD measurements between 10 and 80. SEM was used to analyze the samples that had been prepared (Cam scan MV2300) for their surface morphology and size dispersion. During the SEM investigation, EDS was used to confirm the chemical composition of the final nanostructure. The Philips EM208 microscope was employed to record the TEM micrographs with a 90 kV acceleration voltage.

2.3. Covalent grafting of MTZ to SWCNTs

The pristine SWCNTs were dispersed under robust shaking for 30 h at 70 °C using the HNO3-H2SO4 mixture (1:3 v/v). The obtained product (SWCNT-COOH) was centrifuged at 9000 rpm, washed off and rinsed with DI water, and vacuum-dried at 80 ℃ for 12 h. The dried SWCNT-COOH was suspended using a solution of SoCl2 and DMF, which was then vigorously stirred at 65 °C for 24 h. The next step involved obtaining the product (SWCNT-COCl), washing it with 30 mL of THF, and drying it by vacuum. In subsequent steps, MTZ was used to functionalize SWCNT-COCl. The weight ratio of MTZ-to-SWCNTs (5:1 v/v) was added to a solution of DMF and trimethylamine (1 mL) and stirred for 10 min. SWCNT-COCl and 20 mL of DMF were mixed for 5 min to create the suspension. For 48 h, the suspension was stirred at 120 °C. The extraction of the solid was done after filtering, washing with CH2Cl2 and DI water, and vacuum drying.

2.4. MTZ/SWCNTs/AgNPs synthesis

MTZ/SWCNTs and DI water were mixed for 30 min in the ultrasonic bath. The MTZ/SWCNT dispersion was stirred at room temperature for 30 min after adding a solution of AgNO3 (30 mg) in DI water (10 mL). The suspension mentioned earlier was stirred with 10 mL of NaBH4 for 1 h. Centrifugation, triplicate DI water rinse, and vacuum drying at 50C resulted in the recovery of the desired product, MTZ/SWCNT/AgNP.

2.5. Antibacterial action

2.5.1. Bacterial descents

Antibacterial properties were evaluated on four different types of bacteria using MTZ/SWCNTs/AgNPs: two Gram-negative bacteria (*Escherichia coli* (ATCC 25922) and *Pseudomonas aeruginosa* (ATCC 37853)) and two Gram-Positive strains (*Enterococcus faecalis* (ATCC 29212) and *Staphylococcus aureus* (ATCC 33591)) were utilized for the antibacterial tests. Agar plates were used to keep the cultures at 4 °C. These bacterial strains were chosen based on their unique cell wall composition and structure. Since different studies evaluating nanomaterials have reported that the cell wall composition is strongly linked to antimicrobial activities, an apparent difference in the antibacterial performance of the investigated samples against the considered bacterial strains can be expected.

2.5.2. Investigation of antibacterial activities

For the initial investigation of the antibacterial properties of the nanocomposites, a Kirby-Bauer disc diffusion assay was performed. In summary, the bacterial strains were cultured in a convenient medium. To create a uniform suspension, the bacteria were suspended in a sterile normal saline solution (5 mL) and vortexed. The suspensions were made optically dense enough to have 0.5 McFarland turbidity. The inoculum solution was spread onto a plate that had Muller-Hinton agar with glucose (2 %) using a sterile swab saturated with it. The media inoculated with bacteria received discs containing the determined number of prepared NPs. After incubating it at 37 °C for 24 h, the deterrence zones were analyzed. The measurements were performed in triplicates. By the guidelines of the Clinical Laboratory Standard Institute(CLSI), the minimum repressive condensation MIC and minimum bactericidal concentration MBC were examined using the broth microdilution approach[50].

2.6. Anticancer action

2.6.1. Cell cultivation and growth

The Iranian Biological Resource Center (IBRC) supplied Human gastric adenocarcinoma (AGS) cells that were cultured by the manufacturer's instructions. Dulbecco's Modified Eagle medium nutrient Mixture F-12 (DMEM/F12) was used for cell growth in 25 mL plastic flasks. 10 heat-deactivated foetal bovine serum, 100 U/mL penicillin, and 100 g/mL streptomycin were added to the medium. At 37 °C with 95 % moisture and 5 % CO2, the culture was developed.

2.6.2. Cell livability test

To assess cytotoxicity, mitochondrial activity was evaluated by assessing AGS cells' ability to convert 3-(4,5-dimethyl-thiazol-2-yl)-2,5-diphenyltetrazolium bromide (MTT) to formazan[51]. As a summary, AGS cells were seeded onto 96-well plates at 1 105 cells per well and allowed to grow to 75 % confluence. Different concentrations (0.97, 1.95, 3.9, 7.81, 15.67, 31.25, 125, 250, and 500 μg/mL) of MTZ/SWCNTs/AgNPs were used to treat the cells and they were incubated for 24 h. The negative control consisted of AGS cells cultured for 24 h in a medium lacking MTZ/SWCNTs/AgNPs. The cells were retreated using 10 L of MTT stock mixture (5 mg/mL) and developed for 4 h at 37 °C. After discarding the solution, each well was filled with 100 L of dimethyl sulfoxide, and Each well was coated with 100μ L of DMSO and incubated in the dark for 10 min to dissolve the insoluble formazan crystals. At 570 nm, an ELISA reader was used to measure the absorbance of each well immediately. Using the chemical expression: percentage of livability at each concentration =

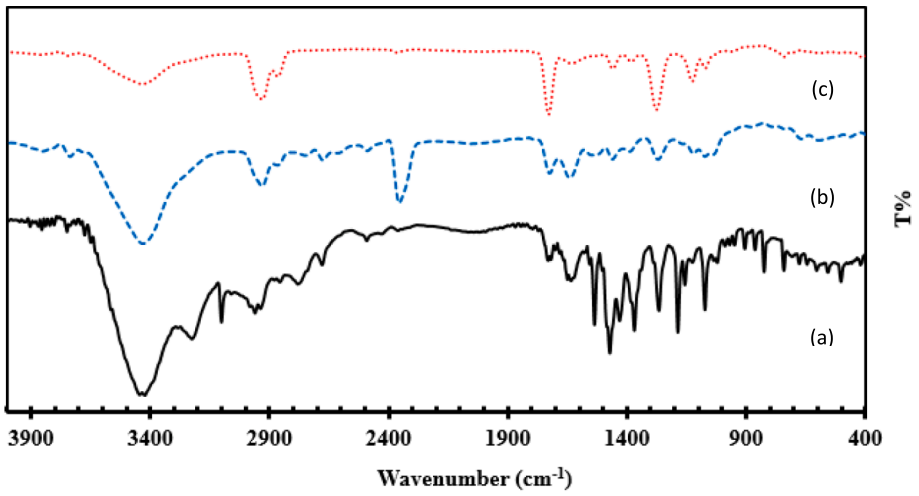

Fig. 1. FTIR spectrum of (a) SWCNTs, b) SWCNTs-COOH, (c) MTZ/SWCNTs/AgNPs.

(corrected mean OD of the test/corrected mean OD of control) × 100, the percentage of viable cells was measured.

2.6.3. Apoptosis assay of MTZ/SWCNTs/AgNPs

Apoptotic activity was defined by employing the Annexin-V-FITC/propidium iodide (PI),while staining kit was used to determine apoptotic activity, based on the manufacturer's guidelines. To sum up, AGS cells underwent a 24-hour treatment with 31.25 g/mL of MTZ/SWCNTs/AgNPs. Following this, the cells were gathered, centrifuged at 200 g, and placed in a proper shock absorber. The compound was developed for 5 min at 25 °C after being treated with 5 L of Annexin-V-FITC labeling solution and 5 L of PI solution and Analysis was done using flow cytometry.

2.7. Morphological analysis

Morphological changes in cell death in AGS cells treated withMTZ/SWCNTs/AgNPs wer-
e observed by observing morphological changes using an inverted microscope. As negative controls, untreated cells were utilized.

2.8. Statistical analysis

The mean and SD of three replicates are used to present the values of each group. $P < 0.05$ was determined as the significance level for the t student −test in data analysis.

3. Findings and discussion

3.1. Synthesis and characterization of MTZ/SWCNTs/AgNPs

MTZ-functionalized SWCNTs were prepared via the reaction of acylated SWCNTs with MTZ. The AgNPs were then deposited on the surface of the MTZ/SWCNTs. In (Scheme 1) the procedure for preparing MTZ/SWCNT/AgNP is explained in detail. FTIR analysis was used to distinguish the functional groups in the obtained samples. Fig. 1 illustrates the FTIR spectrum of SWCNT, SWCNTs-COOH, and MTZ/SWCNTs). The principal feature soaking up band of the SWCNTs is caused by extending quivering of the OH radicals (3600 cm-1).The -COOH group's extending causes the peak at 1710 cm-1, as shown in (Fig. 1b). In addition, the broadband at 3400 cm^{-1} indicates a hydroxyl group, which indicates the successful oxidation of the SWCNTs. Fig. 1c depicts the FTIR spectrum of MTZ/SWCNT, with distinct bands in 1500 and 1610 cm^{-1} that represent the vibrations of the N-C = N and C = N groups,in the order given. The C-H stretching band and the N-O band are visible at 1150 cm^{-1} and 1356 cm^{-1}, indicating that MTZ was properly attached to the SWCNTs surface.

FE-SEM images were utilized to assess the morphological structure of the MTZ/SWCNTs/AgNPs. The FE-SEM images are shown in (Fig. 2). The surfaces of the SWCNTs were covered with MTZ and AgNPs, as shown in (Fig. 2). TEM images were used to investigate the morphology and size distribution of the MTZ/SWCNTs/AgNPs. Fig. 3 illustrates the corresponding TEM micrograph of the MTZ/SWCNTs/AgNPs nanocomposite. As shown in (Fig. 3), this observation proves the successful

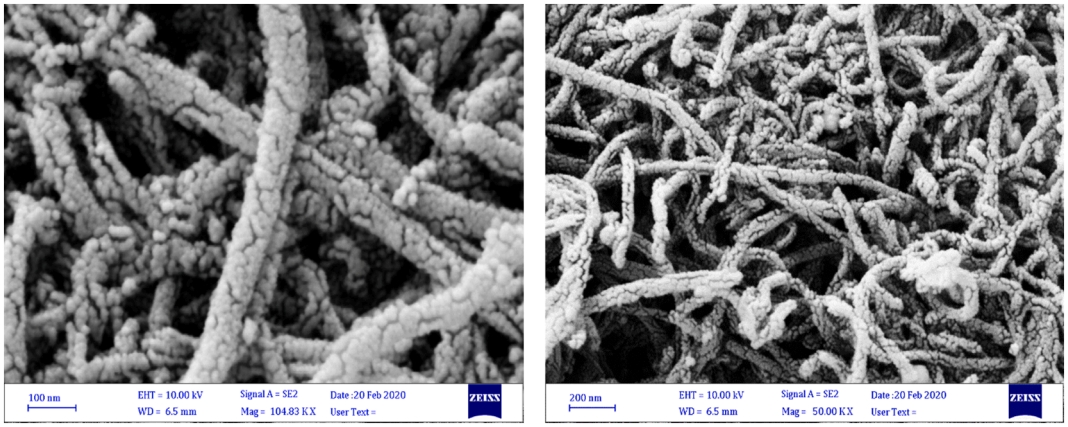

Fig. 2. FE-SEM images of MTZ/SWCNTs/AgNPs with different magnifications.

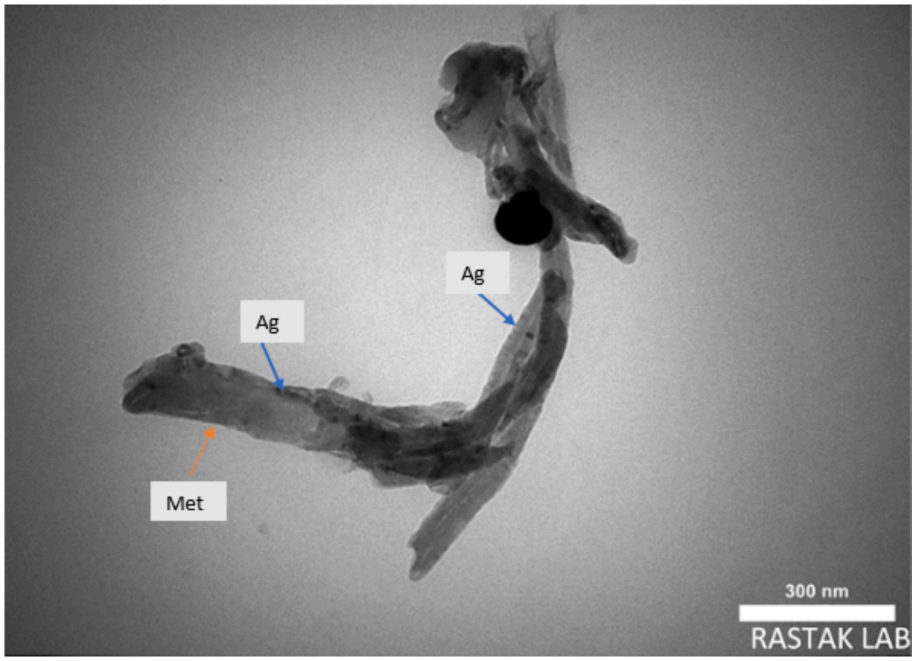

Fig. 3. TEM micrograph of MTZ/SWCNTs/AgNPs nanocomposite.

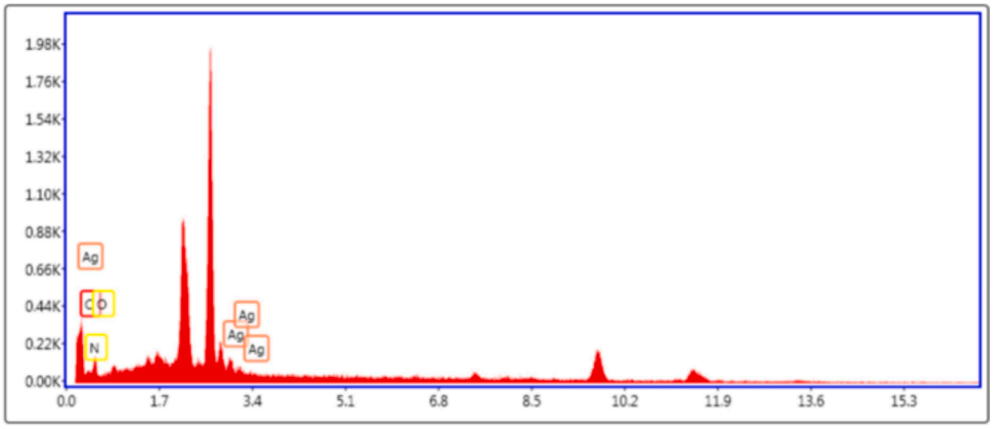

Fig. 4. EDX pattern of MTZ/SWCNTs/AgNPs nanocomposite.

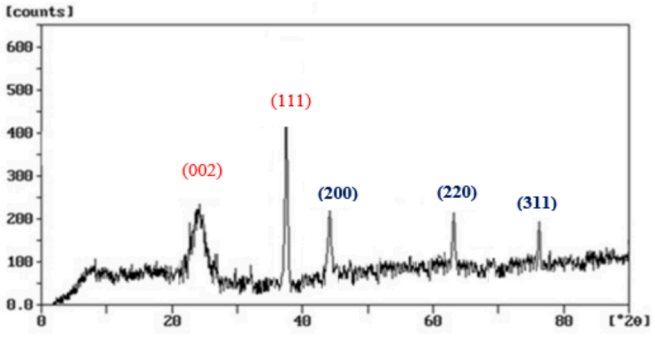

Fig. 5. XRD pattern of MTZ/SWCNTs/AgNPs sample.

decoration of SWCNTs with AgNPs. Importantly, no agglomeration was observed on the modified SWCNT surface.

These results demonstrate the significance of MTZ in improving the uniform distribution of AgNPs. EDS (Fig. 4) was used to determine the elemental composition of the MTZ/SWCNTs/Ag nanocomposite, and the peaks indicate that C, O, N, and Ag atoms were present. The EDX pattern showed that AgNPs were successfully added to the surface of MTZ/SWCNTs. By using wavelength-dispersive X-ray spectroscopy (WDXS), it was possible to confirm the chemical composition of the SWCNTs/AgNPs further. The quantitative maps of C, N, O, and Ag revealed that the nanocomposite had MTZ groups and AgNPs with a suitable dispersion.

The XRD design of the MTZ/SWCNTs/AgNPs sample is presented in (Fig. 5). The emergence of a diffraction peak at $2\theta = 23.8^{\circ}$ was related to the Bragg (0 0 2) plane of hexagonal graphite, indicating that the functionalization of SWCNTs with MTZ/AgNPs did not change the initial crystal structure of the SWCNTs. Metallic Ag's (1 1 1), (2 0 0) (2 2 0), and (3 1 1) Bragg crystallographic planes were believed to be responsible for the apparent diffraction peaks at approximately $2 = 38.2^{\circ}$ and 44.5°, 64.5°, and 77.3° based on their apparent shape. The obtained diffraction pattern proved that the AgNPs were properly deposited on the surface of the MTZ/SWCNTs sample. Furthermore, the XRD pattern confirmed the high purity of the prepared nanocomposite as no additional phases were observed.

Table 1
Inhibition zones of the investigated samples.

Strain	Zone of inhibition		
	MTZ	MTZ/SWCNTs	MTZ/SWCNTs/AgNPs
S. aureus	–	3.1 ± 1	12 Â ± 2
E. coli	–	1.2 ± 2	10 Â ± 4
E. faecalis	–	2.8 ± 4	13.1 ± 1
P. aeruginosa	–	1 ± 3	8.9 ± 2

Table 2
MIC and MBC of MTZ/SWCNTs/AgNPs for different bacterial strains.

Strain	MIC (μg ml^{-1})	MBC (μg ml^{-1})
S. aureus	220	320
E. coli	260	380
E. faecalis	200	320
P. aeruginosa	200	300

3.2. Antibacterial potential

To assess the antibacterial properties, the diameters of the inhibition zones of MTZ, MTZ/SWCNTs, and MTZ/SWCNTs/AgNPs were measured against different bacterial strains (Table 1). Table 2 also displays the MIC and MBC values. Comparing MTZ, MTZ/SWCNTs, and MTZ/SWCNTs/AgNPs' bactericidal concentrations revealed that MTZ/SWCNTs/AgNPs had much lower bactericidal concentrations than MTZ and MTZ/SWCNTs. Xia and coworkers evaluated the antimicrobial properties of the Ag/CNT hybrid against *E. coli* and compared its activity with AgNPs. The prepared AgNPs/CNT exhibited enhanced antimicrobial activity against *E. coli* compared with AgNPs [52]. Additionally, the MTZ/SWCNTs/AgNPs had superior antibacterial efficacy against gram-positive bacteria (*S. aureus* and *E. faecalis*) than against gram-negative bacteria (*E. Coli* and *P.aeroginosa*). In a similar study, the antimicrobial activity of AgNPs-functionalized MWCNTs was investigated for different bacteria, and the prepared nanocomposite was found to be more sensitive to gram-positive bacteria [53]. The current investigation's findings validated previous reports that AgNPs were more effective against gram-positive bacteria than gram-negative bacteria [54,55]. The antibacterial effect of MTZ/SWCNTs/AgNPs was a result of a synergistic effect between both AgNPs and SWCNTs, as confirmed by these results. Furthermore, the agar plate treated with DMF as a positive control did not show an obvious inhibition zone. The bactericidal mechanism of the prepared nanocomposite was attributed to the physical interaction of MTZ/SWCNT/AgNPs with the cell tissue layer based approachand the disturbance of cell function.

3.3. Morphological analysis using an inverted microscope

AGS cells were exposed for 24 h to MTZ/SWCNTs/AgNPs, and an inverted microscope was used to observe morphological changes. Fig. 6A depicts the morphology of the control AGS cells (untreated to MTZ/SWCNTs/AgNPs). After treatment with MTZ/SWCNTs/AgNPs, AGS cells exhibited significant morphological alterations, including granulation and cell rounding (Fig. 6B), which are characteristic of apoptosis.

3.4. Cell viability analysis

The MTT assay was utilized to measure how cytotoxic various concentrations of MTZ/SWCNTs/AgNPs are on AGS cells for 24 h. The MTT assay's Formazan accumulation directly indicates mitochondrial activity in living cells and serves as an indirect indicator of cell viability. Cell viability was decreased in a dose- based approach after MTZ/SWCNTs/AgNPs treatment, as shown in the results. The present findings [56]

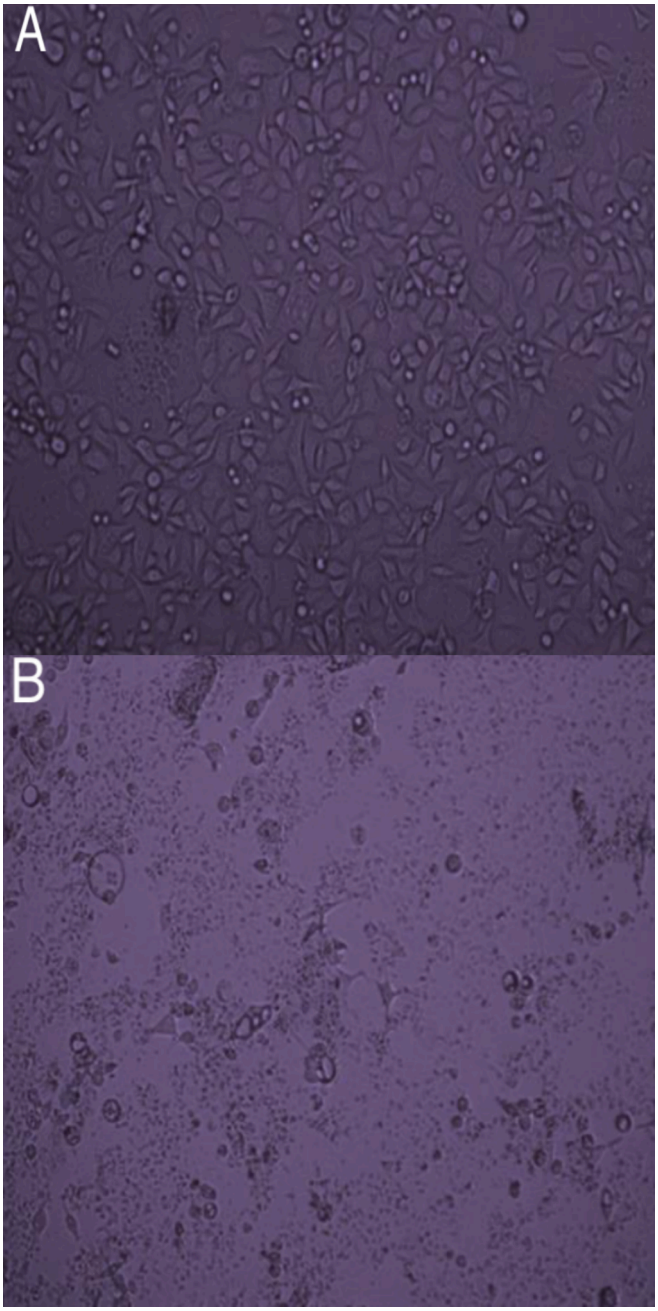

Fig. 6. Morphological changes of MTZ/SWCNTs/AgNPs on AGS cells. The cells (1×10^5 cells/well) were cultured in DMEM/F12 medium supplemented with 10 % heat-inactivated FBS and treated in the absence (control cells) or presence of MTZ/SWCNTs/AgNPs at 31.25 μg/mL for 24 h at 37 °C. Morphological changes of treated cells were observed with an inverted microscope and compared with control cells. Fig. 7B (20X) shows granulation and cell rounding in AGS cells treated with MTZ/SWCNTs/AgNPs as compared to untreated cells (7A, 20X).

indicate that CNTs reduced cancer cell viability dose-dependently. The viability of AGS cells after exposure to 0.97, 1.95, 3.9, 7.81, 15.67, 31.25, 125, 250, and 500 μg/mL of MTZ/SWCNTs/AgNPs was 77, 68, 62, 60, 56, 52, 38, 34, 13, and 6 %, respectively (Fig. 7). According to estimates, the half-maximal inhibitory concentration of AGS is 31.25 g/mL. Yallappa et al. examined the cytotoxic impact of Ag and copper (Cu) biohybrid nanomaterials on a variety of cancerous and normal cell lines. Their findings demonstrated that biohybrid nanomaterials particularly targeted cancer cells and exhibited low cytotoxicity against normal cell

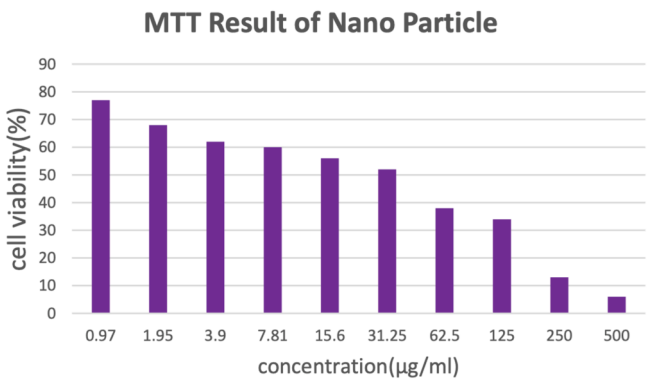

Fig. 7. Cell viability of the AGS cells after treatment with MTZ/SWCNTs/AgNPs. The cytotoxicity was evaluated by the MTT method 24 h after treatment of the cell line with MTZ/SWCNTs/AgNPs (0.97–500 µg/mL).

lines [57].

3.5. The effect of MTZ/SWCNTs/AgNPs on apoptosis and necrosis

Apoptosis cells were determined by the use of an Annexin-V-FITC Apoptosis Detection Kit.

Apoptotic cells were labeled with inverted phosphatidylserine on their cell surface using Annexin-V-FITC, while PI was utilized to detect necrotic cells. After positioning the parts on Annexin-V/PI dot plots, living cells were identified Annexin V−/PI −), primary/early apoptotic cells (Annexin V+/PI −), late apoptotic/secondary apoptotic cells (Annexin V+/PI +), and necrotic cells (Annexin V−/PI +). AGS cells underwent treatment with an IC50 dose (Fig. 8). According to the results, 31.25 µg/mL of MTZ/SWCNTs/AgNPs led to necrosis cell death (12.4 %). The following figure shows the percentages of early (11.9 %) and late (6.94 %) apoptotic cells. The total Q2 and Q3 quadrants of the studied cell population (Fig. 9) are combined in the bar graphs to present the percentage of apoptotic cells) Chen et al. created a CNT-based drug delivery system to deliver 5-fluorouracil (5-FU) to drug-resistant gastric cancer via peritoneal diffusion. The novel drug delivery system was effective in promoting apoptosis of 5-FU-resistant gastric cancer cells, preventing invasion, and improving chemotherapy [58]. In addition, Wen et al. have utilized CNTs to co-deliver the multi-target kinase inhibitor sorafenib and epidermal growth factor receptor small interfering RNA to treat liver cancer [59].

4. Conclusion

This study involved successfully grafting MTZ onto the SWCNT surface and then depositing AgNPs to generate a new antibacterial hybrid material. Utilizing HNO3 and H2SO4, SWCNTs were carboxylated effectively in this method. Subsequently, SWCNTs functionalized with an acidic group can form a strong ester bond with the alcohol agent MTZ. The surface modification of SWCNTs with MTZ groups and AgNPs was confirmed by performing morphological and structural analyses, such as SEM, TEM, FTIR, XRD, and EDX. The antimicrobial characteristics of the MTZ/SWCNTs/AgNPs were better against representative gram-positive bacteria than gram-negative bacteria in this work. We examined the biological significance of MTZ/SWCNTs/AgNPs in gastric cancer treatments. According to our present study, the conjugation of SWCNTs to AgNPs and their modification with MTZ restored the anticancer activity. According to the MTT assay, MTZ/SWCNTs/AgNPs lowered the viability of cancer cells in a dose-responsive manner. The physicochemical properties of MTZ/SWCNTs/AgNPs make them effective in inducing apoptosis in AGS cells, which leads to a reduction in cancer cell viability. Taken together, MTZ/SWCNTs/AgNPs exhibit promise for utilization in the field of biomedicine, specifically as prospective therapeutic agents for antibacterial and anticancer research endeavors. The molecular pathways via which this nanocomposite induces the death of bacterial and cancerous cells need further investigation.

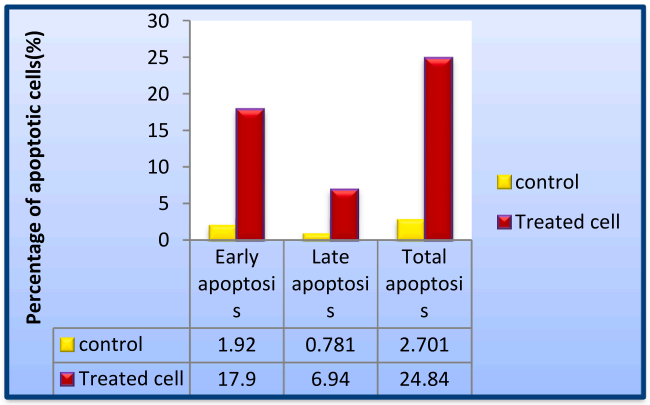

Fig. 9. The bar graphs present the percentage of apoptotic cells.

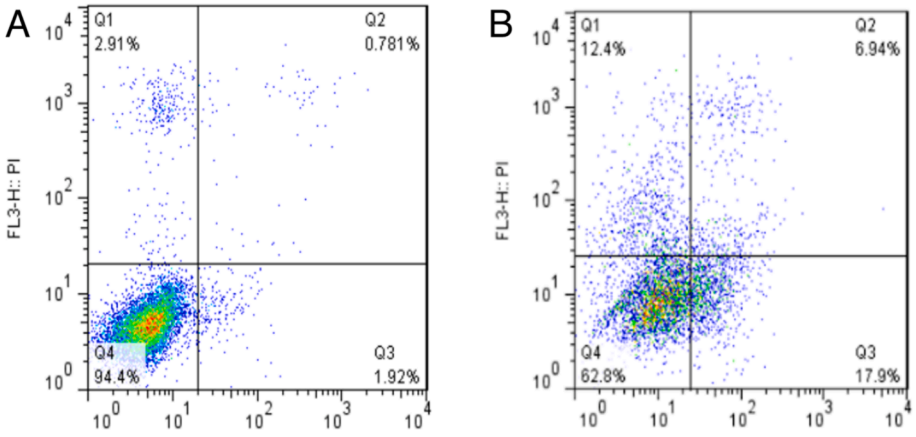

Fig. 8. Evaluation of early and late apoptosis as well as necrosis post-AGS cells post-exposure to MTZ/SWCNTs/AgNPs for 24 h using annexin V-FITC apoptosis detection kit. (A) Control. (B) Treated with MTZ/SWCNTs/AgNPs.

CRediT authorship contribution statement

Shirin Mahmoudi: Writing – review & editing, Writing – original draft, Methodology, Investigation. **Maryam Otadi:** Writing – original draft, Supervision, Funding acquisition, Formal analysis. **Malak Hekmati:** Writing – review & editing, Supervision, Investigation, Formal analysis. **Majid Monajjemi:** Supervision, Methodology, Investigation. **Azadeh Sadat Shekarabi:** Writing – original draft, Methodology, Investigation, Formal analysis.

Declaration of competing interest

The authors declare that they have no known competing financial interests or personal relationships that could have appeared to influence the work reported in this paper.

References

[1] B. Malik, S. Bhattacharyya, Antibiotic drug-resistance as a complex system driven by socio-economic growth and antibiotic misuse, Sci. Rep. 9 (1) (2019) 9788.
[2] Bray, Freddie, et al. "Global cancer statistics 2018: GLOBOCAN estimates of incidence and mortality worldwide for 36 cancers in 185 countries." *CA: a cancer journal for clinicians* 68.6 (2018): 394-424.
[3] F. Prestinaci, P. Pezzotti, A. Pantosti, Antimicrobial resistance: a global multifaceted phenomenon, Pathogens Global Health 109 (7) (2015) 309–318.
[4] J. Hou, et al., Global trend of antimicrobial resistance in common bacterial pathogens in response to antibiotic consumption, J. Hazard. Mater. 442 (2023) 130042.
[5] C. Frick, et al., Quantitative estimates of preventable and treatable deaths from 36 cancers worldwide: a population-based study, Lancet Glob. Health 11 (11) (2023) e1700–e1712.
[6] E.J. Devlin, L.A. Denson, H.S. Whitford, Cancer treatment side effects: a meta-analysis of the relationship between response expectancies and experience, J. Pain Symptom Manage. 54 (2) (2017) 245–258.
[7] M. Arruebo, et al., Assessment of the evolution of cancer treatment therapies, Cancers 3 (3) (2011) 3279–3330.
[8] G. Housman, et al., Drug resistance in cancer: an overview, Cancers 6 (3) (2014) 1769–1792.
[9] M. Nikolaou, et al., The challenge of drug resistance in cancer treatment: a current overview, Clin. Exp. Metastasis 35 (2018) 309–318.
[10] M. Constantin, et al., Synthesis, biological and catalytic activity of silver nanoparticles generated and covered by oxidized pullulan, Mater. Chem. Phys. 295 (2023) 127141.
[11] V. Bordoni, et al., Silver nanoparticles derived by Artemisia arborescens reveal anticancer and apoptosis-inducing effects, Int. J. Mol. Sci. 22 (16) (2021) 8621.
[12] A. Shariati, et al., Graphene-based materials for inhibition of wound infection and accelerating wound healing, Biomed. Pharmacother. 158 (2023) 114184.
[13] C. Dikbas, et al., Green synthesis of silver nanoparticles using common poppy (Papaver rhoeas L.) and evaluation of their potential antibacterial activity, Veterinarska stanica 54 (1) (2023) 47–58.
[14] Abo-Elmahasen, M.M. Fathy, et al., Do silver/hydroxyapatite and zinc oxide nano-coatings improve inflammation around titanium orthodontic mini-screws? In vitro study, Int. Orthod. 21 (1) (2023) 100711.
[15] D. Yang, et al., Characterization of silver nanoparticles loaded chitosan/polyvinyl alcohol antibacterial films for food packaging, Food Hydrocoll. 136 (2023) 108305.
[16] S. Raj, et al., "Specific targeting cancer cells with nanoparticles and drug delivery in cancer therapy.", Semin. Cancer Biol. 69 (2021). Academic Press.
[17] S. Tran, et al., Cancer nanomedicine: a review of recent success in drug delivery, Clin. Transl. Med. 6 (2017) 1–21.
[18] V. Georgakilas, et al., Decorating carbon nanotubes with metal or semiconductor nanoparticles, J. Mater. Chem. 17 (26) (2007) 2679–2694.
[19] P.R. Unwin, A.G. Guell, G. Zhang, Nanoscale electrochemistry of sp2 carbon materials: from graphite and graphene to carbon nanotubes, Acc. Chem. Res. 49 (9) (2016) 2041–2048.
[20] H. Zare, et al., Carbon nanotubes: smart drug/gene delivery carriers, Int. J. Nanomed. (2021) 1681–1706.
[21] Q.-J. Lin, et al., LyP-1-fMWNTs enhanced targeted delivery of MBD1siRNA to pancreatic cancer cells, J. Cell Mol. Med. 24 (5) (2020) 2891–2900.
[22] J.-W. Wang, et al., Neutron activated 153Sm sealed in carbon nanocapsules for in vivo imaging and tumor radiotherapy, ACS Nano 14 (1) (2019) 129–141.
[23] M. Zaboli, H. Raissi, M. Zaboli, Investigation of nanotubes as the smart carriers for targeted delivery of mercaptopurine anticancer drug, J. Biomol. Struct. Dyn. 40 (10) (2022) 4579–4592.
[24] S. Sargazi, et al., Aptamer-conjugated carbon-based nanomaterials for cancer and bacteria theranostics: a review, Chem. Biol. Interact. 361 (2022) 109964.
[25] M. Karimi, et al., Carbon nanotubes part I: preparation of a novel and versatile drug-delivery vehicle, Expert Opin. Drug Deliv. 12 (7) (2015) 1071–1087.
[26] N.X. Dinh, et al., Decoration of silver nanoparticles on multiwalled carbon nanotubes: antibacterial mechanism and ultrastructural analysis, J. Nanomater. 16 (1) (2015) 63.
[27] G. Shaham, H. Veisi, M. Hekmati, Silver nanoparticle-decorated multiwalled carbon nanotube/pramipexole nanocomposite: Synthesis, characterization and application as an antibacterial agent, Appl. Organomet. Chem. 31 (10) (2017) e3737.
[28] B. Li, et al., Effective deactivation of A549 tumor cells in vitro and in vivo by RGD-decorated chitosan-functionalized single-walled carbon nanotube loading docetaxel, Int. J. Pharm. 543 (1-2) (2018) 8–20.
[29] S.-W. Kim, et al., PEGylated anticancer-carbon nanotubes complex targeting mitochondria of lung cancer cells, Nanotechnology 28 (46) (2017) 465102.
[30] D. Liu, et al., "Hyaluronic acid-coated single-walled carbon nanotubes loaded with doxorubicin for the treatment of breast cancer.", Die Pharmazie-An Int. J. Pharm. Sci. 74 (2) (2019) 83–90.
[31] Y. Yan, et al., Stacking of doxorubicin on folic acid-targeted multiwalled carbon nanotubes for in vivo chemotherapy of tumors, Drug Deliv. 25 (1) (2018) 1607–1616.
[32] D.h.S. Ahmed, M.KA. Mohammed, M.R. Mohammad, Sol–gel synthesis of Ag-doped titania-coated carbon nanotubes and study their biomedical applications, Chem. Pap. 74 (1) (2020) 197–208.
[33] W. Wu, et al., Covalently combining carbon nanotubes with anticancer agent: preparation and antitumor activity, ACS Nano 3 (9) (2009) 2740–2750.
[34] Abousalman-Rezvani, Zahra, et al. "Functionalization of carbon nanotubes by combination of controlled radical polymerization and "grafting to" method." *Advances in colloid and interface science* 278 (2020): 102126.
[35] K. Venugopal, et al., Synthesis of silver nanoparticles (Ag NPs) for anticancer activities (MCF 7 breast and A549 lung cell lines) of the crude extract of Syzygium aromaticum, J. Photochem. Photobiol. B Biol. 167 (2017) 282–289.
[36] Y. He, et al., Biosynthesis, antibacterial activity and anticancer effects against prostate cancer (PC-3) cells of silver nanoparticles using Dimocarpus Longan Lour. peel extract, Nanoscale Res. Lett. 11 (2016) 1–10.
[37] D. Nayak, et al., Biologically synthesised silver nanoparticles from three diverse family of plant extracts and their anticancer activity against epidermoid A431 carcinoma, J. Colloid Interface Sci. 457 (2015) 329–338.
[38] T.V.M. Sreekanth, et al., Green synthesis: in-vitro anticancer activity of silver nanoparticles on human cervical cancer cells, J. Clust. Sci. 27 (2016) 671–681.
[39] Alsalhi, S. Mohamad, et al., "Green synthesis of silver nanoparticles using Pimpinella anisum seeds: antimicrobial activity and cytotoxicity on human neonatal skin stromal cells and colon cancer cells.", Int. J. Nanomed. (2016) 4439–4449.
[40] B. Kumar, et al., In vitro evaluation of silver nanoparticles cytotoxicity on Hepatic cancer (Hep-G2) cell line and their antioxidant activity: Green approach for fabrication and application, J. Photochem. Photobiol. B Biol. 159 (2016) 8–13.
[41] M.S. Jabir, et al., Functionalized SWCNTs@ Ag–TiO2 nanocomposites induce ROS-mediated apoptosis and autophagy in liver cancer cells, Nanotechnol. Rev. 12 (1) (2023) 20230127.
[42] R. Rajendran, A. Mani, Photocatalytic, antibacterial and anticancer activity of silver-doped zinc oxide nanoparticles, J. Saudi Chem. Soc. 24 (12) (2020) 1010–1024.
[43] P. Das, et al., Interaction of flavonols with human serum albumin: A biophysical study showing structure–activity relationship and enhancement when coated on silver nanoparticles, J. Biomol. Struct. Dyn. 37 (6) (2019) 1414–1426.
[44] A.K. Shukla, et al., Selective ion removal and antibacterial activity of silver-doped multi-walled carbon nanotube/polyphenylsulfone nanocomposite membranes, Mater. Chem. Phys. 233 (2019) 102–112.
[45] D.i. Huang, et al., Ag nanoparticles decorated electrospinning carbon nanotubes/polyamide nanofibers, J. Biomater. Sci. Polym. Ed. 30 (18) (2019) 1744–1755.
[46] S.-H. Uhm, et al., Tailoring of antibacterial Ag nanostructures on TiO2 nanotube layers by magnetron sputtering, J. Biomed. Mater. Res. B Appl. Biomater. 102 (3) (2014) 592–603.
[47] S. Abdelnasir, et al., Metronidazole conjugated magnetic nanoparticles loaded with amphotericin B exhibited potent effects against pathogenic Acanthamoeba castellanii belonging to the T4 genotype, AMB Express 10 (2020) 1–11.
[48] D. Żyro, et al., Multifunctional Silver (I) complexes with metronidazole drug reveal antimicrobial properties and antitumor activity against human hepatoma and colorectal adenocarcinoma cells, Cancers 14 (4) (2022) 900.
[49] M. Kawamoto, et al., Combined gemcitabine and metronidazole is a promising therapeutic strategy for cancer stem-like cholangiocarcinoma, Anticancer Res 38 (5) (2018) 2739–2748.
[50] Cockerill, Franklin R., et al. "Clinical and laboratory standards institute." *Performance standards for antimicrobial susceptibility testing: twenty-second informational supplement* (2012).
[51] T. Mosmann, Rapid colorimetric assay for cellular growth and survival: application to proliferation and cytotoxicity assays, J. Immunol. Methods 65 (1-2) (1983) 55–63.
[52] L. Xia, et al., Facile construction of Ag nanoparticles encapsulated into carbon nanotubes with robust antibacterial activity, Carbon 130 (2018) 775–781.
[53] V.K. Rangari, et al., Synthesis of Ag/CNT hybrid nanoparticles and fabrication of their nylon-6 polymer nanocomposite fibers for antimicrobial applications, Nanotechnology 21 (9) (2010) 095102.
[54] P.B. Dayma, et al., Synthesis of bio-silver nanoparticles using desert isolated Streptomyces intermedius and its antimicrobial activity, J. Pharm. Chem. Biol. Sci 7 (2019) 94–101.
[55] A. Bakhtiari-Sardari, et al., Comparative evaluation of silver nanoparticles biosynthesis by two cold-tolerant Streptomyces strains and their biological activities, Biotechnol. Lett 42 (2020) 1985–1999.
[56] B.F. Dizaji, et al., The role of single-and multi-walled carbon nanotube in breast cancer treatment, Ther. Deliv. 11 (10) (2020) 653–672.

[57] S. Yallappa, et al., Phytochemically functionalized Cu and Ag nanoparticles embedded in MWCNTs for enhanced antimicrobial and anticancer properties, Nano-micro letters 8 (2016) 120–130.
[58] W. Chen, et al., Construction of aptamer-siRNA chimera/PEI/5-FU/carbon nanotube/collagen membranes for the treatment of peritoneal dissemination of drug-resistant gastric cancer, Adv. Healthc. Mater. 9 (21) (2020) 2001153.
[59] Z. Wen, et al., Multiwalled carbon nanotubes co-delivering sorafenib and epidermal growth factor receptor siRNA enhanced tumor-suppressing effect on liver cancer, Aging (Albany NY) 13 (2) (2021) 1872.